An Equivalent Circuit Model of Living Myocardial Slice Cultured on Microelectrode Array with in-vitro Experimental Validations

Guan, Rui; Shen, Tao; Knops, Paul; Taverne, Yannick J.H.J.; Gao, Zhenyu; Du, Sijun; Van Veldhoven, Robert; De Groot, Natasja M.S.; Widdershoven, Frans

DOI
10.1109/BioCAS61083.2024.10798316

Publication date
2024

Document Version
Final published version

Published in
2024 IEEE Biomedical Circuits and Systems Conference, BioCAS 2024

2024 IEEE Biomedical Circuits and Systems Conference (BioCAS) | 979-8-3503-5495-9/24/$31.00 ©2024 IEEE | DOI: 10.1109/BioCAS61083.2024.10798316

An Equivalent Circuit Model of Living Myocardial Slice Cultured on Microelectrode Array with in-vitro Experimental Validations

Rui Guan[1,2,3], Tao Shen[1], Paul Knops[2], Yannick J. H. J. Taverne[4],
Zhenyu Gao[5], Sijun Du[1], Robert van Veldhoven[3], Natasja M. S. De Groot[2,1], Frans Widdershoven[3,1]
[1]*Department of Microelectronics, Delft University of Technology,* Delft, the Netherlands
[2]*Department of Cardiology, Erasmus University Medical Center,* Rotterdam, the Netherlands
[3]*NXP Semiconductors,* Eindhoven, the Netherlands
[4]*Department of Cardiothoracic Surgery, Erasmus University Medical Center,* Rotterdam, the Netherlands
[5]*Department of Neuroscience, Erasmus University Medical Center,* Rotterdam, the Netherlands
Email: rui.guan@nxp.com

***Abstract*—In this paper, we present an equivalent circuit model that integrates a living myocardial slice (LMS) cultured on a microelectrode array (MEA) to effectively simulates a heart-on-a-chip (HoC) within Electronic Design Automation (EDA) software. The cardiac fiber model consists of cardiomyocytes interconnected by gap junctions to simulate the action potential (AP) conduction in the longitudinal direction. We systematically explored several parameters, including gap junction resistors, seal resistors, and electrode diameters, to assess their effects on local field potential (LFP). The model accuracy was validated through *in vitro* experiments using mouse LMS, confirming its potential for guiding HoC design in cardiac research.**

***Index Terms*—heart-on-a-chip (HoC), microelectrode array (MEA), action potential (AP), local field potential (LFP), Verilog-A model, living myocardial slice (LMS).**

I. Introduction

In recent years, the heart-on-a-chip (HoC) platform, as depicted in Fig. 1, has emerged as a promising technology for drug screening and disease modeling applications [1]. To measure electrical signals of the *in vitro* cardiomyocytes, the CMOS-based microelectrode array (MEA) is a widespread tool with highlights of high throughput, free label, and high frame rate, compared with traditional commercial electrophysiology tools such as patch clamp and fluorescence imaging [2].

To design a HoC platform for investigating heart arrhythmias, several research groups have introduced the circuit models of cardiomyocyte membrane, utilizing data from patch clamp experiments [3], [4]. However, heart arrhythmias are not only associated with abnormal action potential (AP) but also disorders of AP conduction. Some researchers have investigated the model of cardiac fibers by positioning a gap junction between adjacent cardiomyocytes [5], [6]. Still, living myocardial slice (LMS) experiments were missing to validate their models. Moreover, there is an unmet need to simulate the biological behaviors of LMS together with MEA within electronic design automation (EDA) software [7], as the model can provide valuable instructions to design an MEA with proper specifications and predict the chip performance before costly and time-consuming fabrications.

This research was funded in part by the Medical Delta Cardiac Arrhythmia Lab (CAL), The Netherlands.

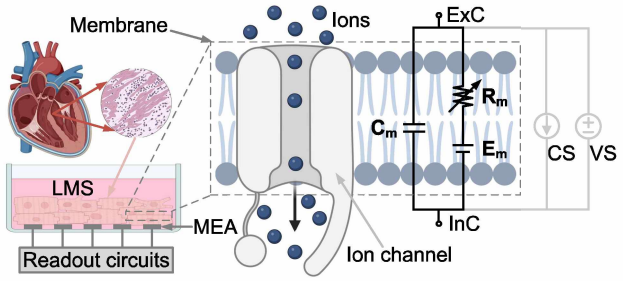

Fig. 1: The conceptual diagram of heart-on-a-chip (HoC) and simplified equivalent circuit model of cardiomyocyte membrane.

To overcome the above-mentioned challenges, this paper proposes an integrated circuit model of one-dimensional (1-D) human cardiac fiber cultured on an MEA. The computationally efficient mathematical electrophysiological model of a single ventricular cell [3] in Fig. 1 was implemented with Verilog-A model with two terminals, intracellular (InC) and extracellular (ExC), and the gap junction was modeled as one resistor to simulate the APs conduction between adjacent cardiomyocytes [5], [6]. The electrode-tissue interface (ETI) model bridges the gap between cardiomyocytes and AC-coupled recording systems. The local field potentials (LFPs) were simulated with this equivalent circuit model of HoC in Cadence. Moreover, we conducted *in vitro* experiments with mouse LMS [8], [9] for model verification. The flexible MEA with 64 electrodes was fabricated to increase the seal resistor by improving the contact between contracting LMS and electrodes, enhancing the signal-to-noise ratio (SNR).

In Section II, the Verilog-A model of the cardiomyocyte membrane is introduced, and the equivalent circuit model of 1-D cardiac fiber cultured on an MEA is shown in Section

III. In Section IV, the *in vitro* mouse LMS test results are described, followed by a conclusion in Section V.

II. MODEL OF CARDIOMYOCYTE MEMBRANE

The cardiomyocyte membrane can be effectively modeled as a cell membrane capacitor, C_m, in parallel with a time-varying resistor, R_m, which represents the average effect of voltage-gated ion channels, as depicted in Fig. 1. The equilibrium potential of ion distributions inside and outside the cell is modeled as the DC voltage potential E_m. To implement this concept, we have translated the voltage-current mathematical relations of cell membrane into a Verilog-A model with two terminals, InC and ExC, so it can be used as one electrical component to be seamlessly simulated together with an MEA in Electronic design automation (EDA) software Cadence.

The InC APs can be simulated with a piece of the cell membrane under the current clamp condition, as shown in Fig. 1. The pulsed stimulation current source (CS) flows from ExC to InC to depolarize the cell membrane and trigger APs, and the stimulation threshold should be reached to excite the cells with programmable current pulse amplitude (PA) and pulse width (PW). The results with a cell membrane area of $1000\,\mu m^2$ are shown in Fig. 2(a). The rhythm of generated APs corresponds directly with the CS frequency of 1 Hz with an action potential duration APD_{90} of approximately 356 ms.

The voltage clamp simulations were also performed to investigate the cell membrane property further, and the voltage source (VS) was connected with InC and ExC terminals of the cell membrane. The cell membrane potential was biased at its resting membrane potential (RMP) of $-90.1\,mV$, and increased to $-40\,mV$ and $-20\,mV$ with the interval of 2 s respectively. The rising time T_r and falling time T_f are both 1 ms. The simulated results of cell membrane current I_m is shown in Fig. 2(b).

Due to the varying convergence accuracy of different computation simulators, the values of RMP and APD_{90} in this paper are slightly different from those reported in [3].

III. MODEL OF CARDIAC FIBER CULTURED ON MEA

The 1-D cardiac fiber was modeled with cardiomyocytes and interconnected gap junctions, as shown in Fig. 3(a). As spontaneous APs are not inherent in EDA software, the APs are triggered by a CS applied to an additional cell connected in series to the first cell of the fiber [5], which is the source in Fig. 3(a). Fig. 3(b) illustrates the equivalent circuit model of 1-D cardiac fiber with 2 cells cultured on the MEA as an example. To simplify our model, we overlook the AP conduction within one individual cardiomyocyte. The gap junction was simplified as one resistor R_g without sacrificing the main functionality of AP conduction in [6]. Here, the left half part of the cell membrane interfaces with the cell culture solution, and it is grounded via a silver/silver chloride (Ag/AgCl) electrode. While the resting half-cell membrane in contact with the microelectrode (ME) is depicted as the right part of the model.

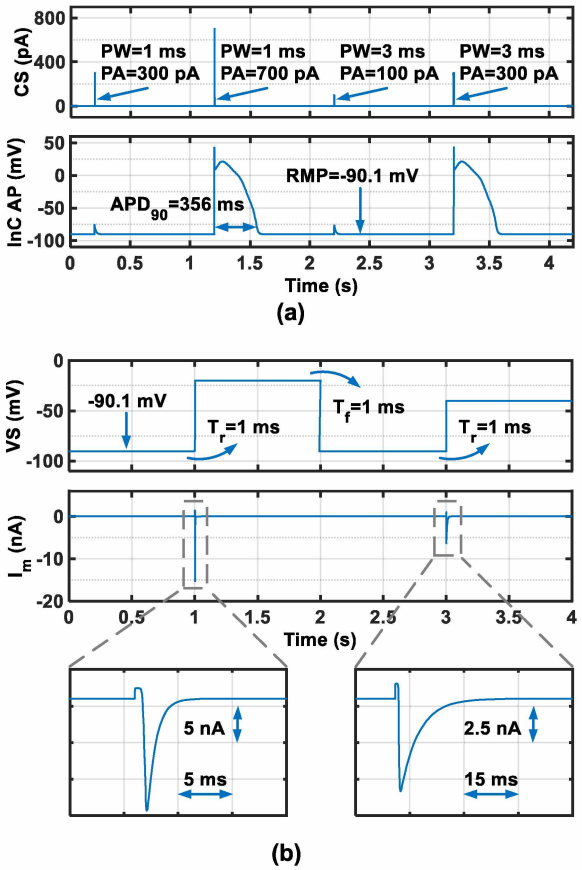

Fig. 2: Simulations of cardiomyocyte membrane (a) in current clamp condition and (b) in voltage clamp condition.

In this paper, the cylindrical human ventricular cell is assumed to have a diameter of 20 µm and a length of 100 µm [10].

In Fig. 3, R_s represents the seal resistor describing how tightly the LMS is attached to the ME. For LMS measurement, the average distance between LMS and ME was assumed in the order from 0.1 µm to 10 µm smaller than a single cell diameter [2], because the LMS can not be attached to ME as closely as in the case of cell culture when cells are grown on MEA. Consequently, R_s was estimated to be from 50 kΩ to 5 MΩ with equation reported in [7], [11], [12].

Transitioning from biological networks to electrical components, we incorporate an ETI model [13]–[15] which encompasses a double layer capacitor (C_{dl}) in parallel with a Faraday resistor (R_F), and the electrode DC offset (V_{DC}) in series with them. With respect of electrode material and area, we estimate C_{dl} and R_F are in the range from 1 nF to 100 nF and 1 MΩ to 10 kΩ respectively.

The LFP signals are captured by an AC-coupled amplifier with bandwidth from 0.5 Hz to 400 Hz [16], which effectively filters out V_{DC}. The C_{in} was 10 pF to meet the input impedance specification, while the C_{fb} was 50 fF to achieve the gain of 200. The high pass corner of 0.5 Hz was created by the C_{fb} and R_{fb} of 6.4 TΩ made of pseudo resistor [17].

In the simulation results with different gap junction resistors

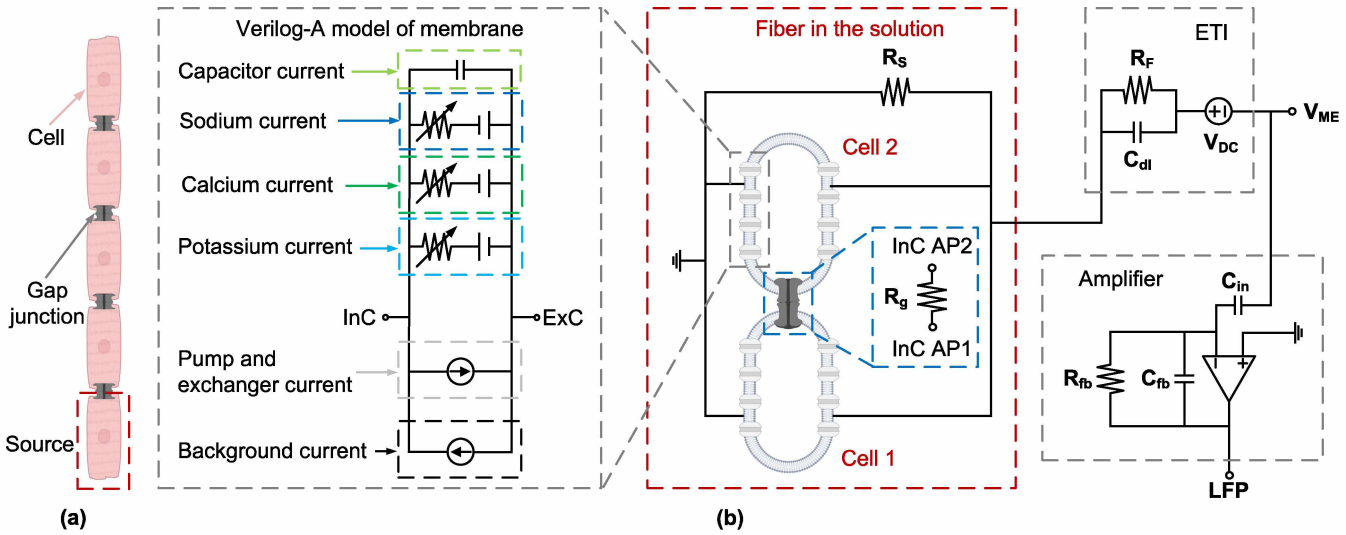

Fig. 3: The 1-D cardiac fiber connection in (a) and (b) the equivalent circuit model of it with 2 cells cultured on MEA.

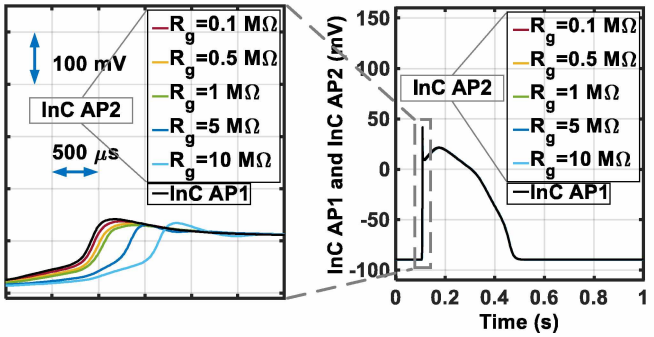

Fig. 4: The simulated InC AP1 and its interconnected cell response InC AP2 with different gap junction resistor (R_g).

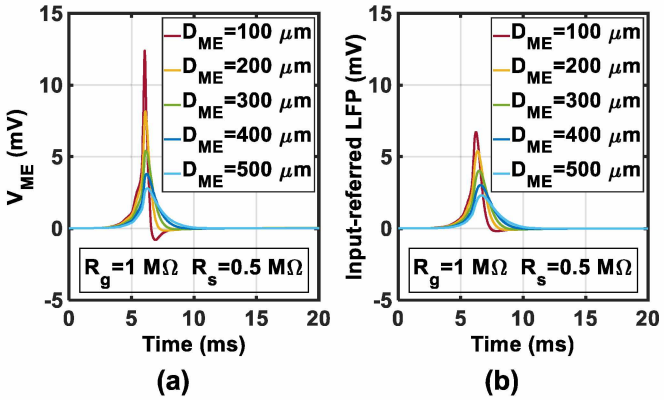

Fig. 5: The simulated V_{ME} and input-referred LFP with different electrode diameter (D_{ME}).

from 0.1 MΩ to 10 MΩ [5], [6] presented in Fig. 4, the black color represents the InC AP1 signal of cell 1 in Fig. 3, which conducts to its interconnected cell 2 via a gap junction, and the response InC AP2 of cell 2 is as shown in 5 other colored APs. The AP conduction speed is decreased with a higher gap

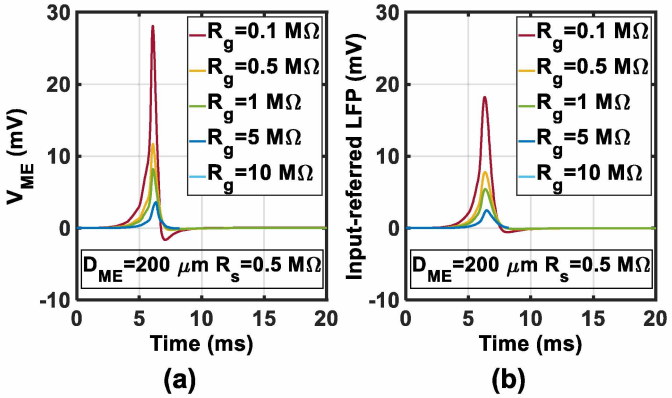

Fig. 6: The simulated V_{ME} and input-referred LFP with different gap junction resistor (R_g).

junction resistor.

The relations of ME voltage (V_{ME}) and input-referred (IR) LFP (which is LFP divided by the amplifier gain) with the circular electrode diameter (D_{ME}) were investigated in Fig. 5. Their amplitude decreases but duration increases with a larger ME because it captures the average signal from more cells, and each cell signal with its own conduction delay. In Fig. 6, the influence of the gap junction resistor on V_{ME} and IR LFP is shown, when D_{ME} is 200 μm. The signal amplitude increases with the smaller R_g, which relates to the higher conduction speed of APs. Additionally, the effect of seal resistor was also explored, V_{ME} and IR LFP amplitude increases dramatically with higher seal resistor as illustrated in Fig. 7. Thus, ensuring close contact between LMS and MEs is crucial for LFP recording with a high seal resistor.

IV. EXPERIMENTAL RESULTS

To validate our model concept, we conducted *in vitro* experiments using mouse ventricular LMS because of their

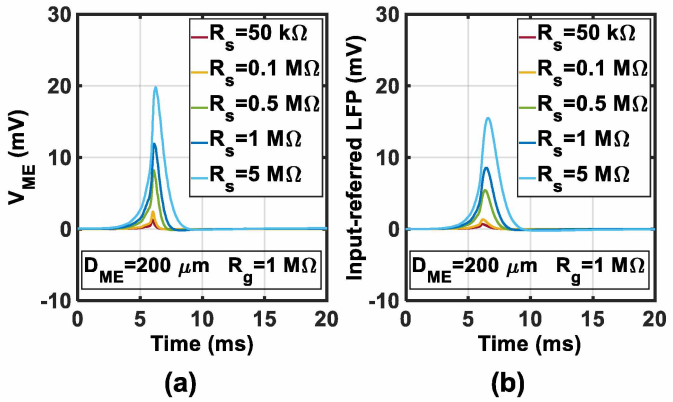

Fig. 7: The simulated V_{ME} and input-referred LFP with different seal resistor (R_s).

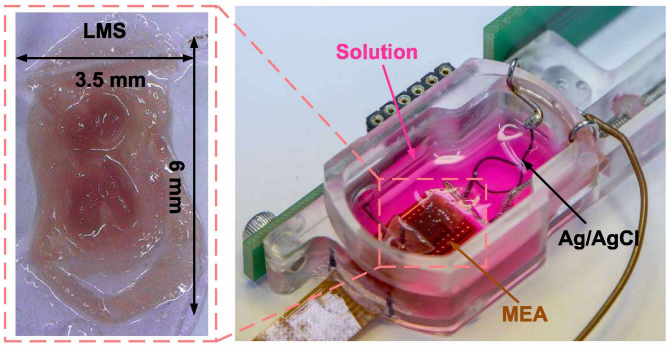

Fig. 8: The experiment setup for *in vitro* LMS measurements.

similarity to mimic human LMS and cost effectiveness [18]–[20]. The experiment setup, along with the LMS, is shown in Fig. 8. In the setup, we use the Ag/AgCl electrode to bias the cell culture solution at ground value and the LMS is cultured on MEA at the bottom of the chamber.

For LFPs recording, we use a commercial application-specific integrated circuit (ASIC) chip (RHD2164, Intan Technologies) to amplify and digitize the signals. It has 64 channels of AC-coupled recording amplifiers with a gain of 192, and a 16-bit successive approximation register (SAR) analog-to-digital converter (ADC) is shared by 64 channels with a time-multiplexer (MUX). The system architecture is shown in Fig. 9(a). The 64-pixel planar circle MEs were fabricated using gold material, and each pixel features a pitch of 950 μm with a diameter of 250 μm and its image is shown in Fig. 9(b). Additionally, the 2 large reference MEs at the boundary of the MEA could be used for bipolar or differential recording to minimize the common mode environmental interference, such as 50/60 Hz noise. Fig. 9(c) shows the impedance measurements of 64 MEs at 100 Hz in the cell culture solution.

The measured LFPs are shown in Fig. 10 over a time period of 20 s. The 4 detailed LFP signals exhibit a duration of approximate 10 ms, closely aligning with the simulation results in Fig.7. However, the slight amplitude discrepancies could be attributed to different cardiomyocyte size of mouse and human, and some estimation errors of the cell-to-electrode distance

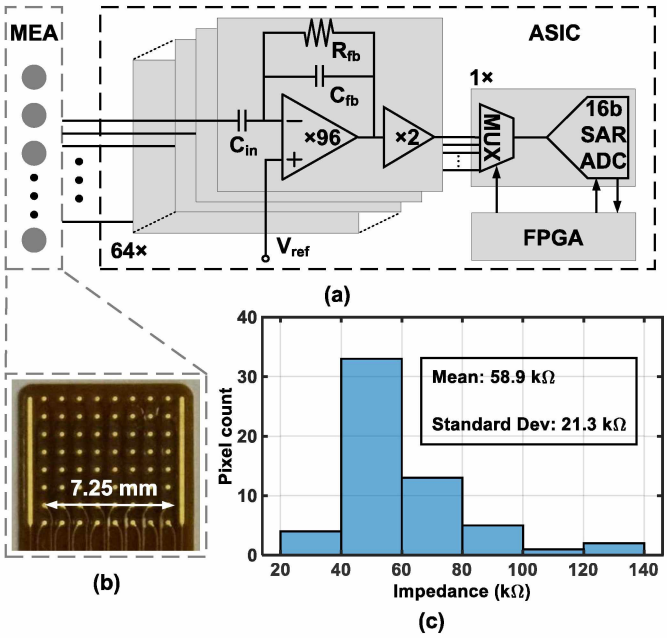

Fig. 9: The circuit diagram of 64-channel LFPs recording system with flexible MEA in (a) and (b), and the histogram of impedance measurements of 64 MEs in (c).

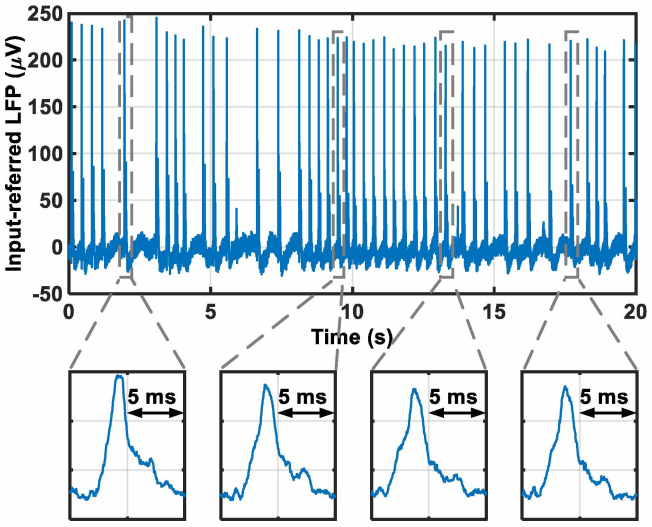

Fig. 10: The measured input-referred LFPs of mouse LMS.

due to LMS contraction and surface overlap coefficient in case a small portion of ME covered by cardiomyocytes [11], [12].

V. CONCLUSION

This paper presents an equivalent circuit model of a 1-D human cardiac fiber cultured on MEA within the commercial chip design software Cadence, it includes the cardiomyocytes, gap junctions, ETI, and AC-coupled LFP readout systems. This model can be extended to other EDA software platforms like PSPICE, HSPICE, and ELDO, etc. The experiment results with mouse LMS validate the accuracy and validity of the proposed model.

REFERENCES

[1] P. R. Van Gorp, S. A. Trines, D. A. Pijnappels, and A. A. De Vries, "Multicellular in vitro models of cardiac arrhythmias: focus on atrial fibrillation," *Frontiers in Cardiovascular Medicine*, vol. 7, p. 43, 2020.

[2] M. E. Spira and A. Hai, "Multi-electrode array technologies for neuroscience and cardiology," *Nature nanotechnology*, vol. 8, no. 2, pp. 83–94, 2013.

[3] O. Bernus, R. Wilders, C. W. Zemlin, H. Verschelde, and A. V. Panfilov, "A computationally efficient electrophysiological model of human ventricular cells," *American Journal of Physiology-Heart and Circulatory Physiology*, vol. 282, no. 6, pp. H2296–H2308, 2002.

[4] M. Courtemanche, R. J. Ramirez, and S. Nattel, "Ionic mechanisms underlying human atrial action potential properties: insights from a mathematical model," *American Journal of Physiology-Heart and Circulatory Physiology*, vol. 275, no. 1, pp. H301–H321, 1998.

[5] S. Rohr, "Role of gap junctions in the propagation of the cardiac action potential," *Cardiovascular research*, vol. 62, no. 2, pp. 309–322, 2004.

[6] A. P. Henriquez, R. Vogel, B. J. Muller-Borer, C. S. Henriquez, R. Weingart, and W. E. Cascio, "Influence of dynamic gap junction resistance on impulse propagation in ventricular myocardium: a computer simulation study," *Biophysical journal*, vol. 81, no. 4, pp. 2112–2121, 2001.

[7] G. Massobrio, S. Martinoia, and P. Massobrio, "Equivalent circuit of the neuro-electronic junction for signal recordings from planar and engulfed micro-nano-electrodes," *IEEE Transactions on Biomedical Circuits and Systems*, vol. 12, no. 1, pp. 3–12, 2017.

[8] J. H. Amesz, L. Zhang, B. R. Everts, N. M. De Groot, and Y. J. Taverne, "Living myocardial slices: Advancing arrhythmia research," *Frontiers in Physiology*, vol. 14, p. 1076261, 2023.

[9] F. G. Pitoulis, S. A. Watson, F. Perbellini, and C. M. Terracciano, "Myocardial slices come to age: an intermediate complexity in vitro cardiac model for translational research," *Cardiovascular Research*, vol. 116, no. 7, pp. 1275–1287, 2020.

[10] R. E. Tracy, G. E. Sander *et al.*, "Histologically measured cardiomyocyte hypertrophy correlates with body height as strongly as with body mass index," *Cardiology research and practice*, vol. 2011, 2011.

[11] S. Martinoia, P. Massobrio, M. Bove, and G. Massobrio, "Cultured neurons coupled to microelectrode arrays: circuit models, simulations and experimental data," *IEEE transactions on biomedical engineering*, vol. 51, no. 5, pp. 859–863, 2004.

[12] P. Massobrio, G. Massobrio, and S. Martinoia, "Interfacing cultured neurons to microtransducers arrays: a review of the neuro-electronic junction models," *Frontiers in neuroscience*, vol. 10, p. 177927, 2016.

[13] A. Wang, D. Jung, J. Park, G. Junek, and H. Wang, "Electrode–electrolyte interface impedance characterization of ultra-miniaturized microelectrode arrays over materials and geometries for sub-cellular and cellular sensing and stimulation," *IEEE Transactions on NanoBioscience*, vol. 18, no. 2, pp. 248–252, 2019.

[14] W. Franks, I. Schenker, P. Schmutz, and A. Hierlemann, "Impedance characterization and modeling of electrodes for biomedical applications," *IEEE Transactions on Biomedical Engineering*, vol. 52, no. 7, pp. 1295–1302, 2005.

[15] J. Guo, J. Yuan, and M. Chan, "Modeling of the cell-electrode interface noise for microelectrode arrays," *IEEE Transactions on Biomedical Circuits and Systems*, vol. 6, no. 6, pp. 605–613, 2012.

[16] A. Yaksh, L. J. van der Does, C. Kik, P. Knops, F. B. Oei, P. C. van de Woestijne, J. A. Bekkers, A. J. Bogers, M. A. Allessie, and N. M. de Groot, "A novel intra-operative, high-resolution atrial mapping approach," *Journal of Interventional Cardiac Electrophysiology*, vol. 44, pp. 221–225, 2015.

[17] R. R. Harrison and C. Charles, "A low-power low-noise cmos amplifier for neural recording applications," *IEEE Journal of solid-state circuits*, vol. 38, no. 6, pp. 958–965, 2003.

[18] S. Kaese and S. Verheule, "Cardiac electrophysiology in mice: a matter of size," *Frontiers in physiology*, vol. 3, p. 345, 2012.

[19] T. O'Hara and Y. Rudy, "Quantitative comparison of cardiac ventricular myocyte electrophysiology and response to drugs in human and nonhuman species," *American Journal of Physiology-Heart and Circulatory Physiology*, vol. 302, no. 5, pp. H1023–H1030, 2012.

[20] N. B. Robinson, K. Krieger, F. M. Khan, W. Huffman, M. Chang, A. Naik, R. Yongle, I. Hameed, K. Krieger, L. N. Girardi *et al.*, "The current state of animal models in research: A review," *International Journal of Surgery*, vol. 72, pp. 9–13, 2019.